



Molecular sieve-supported ionic liquids as efficient adsorbents for CO₂ capture

NA YANG¹ and RUI WANG^{2*}

¹School of Environmental Science and Engineering, Shandong University, Jinan 250100, Shandong, China, E-mail: yangna13579@tom.com and ²School of Environmental Science and Engineering, Shandong University, Jinan 250100, Shandong, China

(Received 22 February, revised 29 September 2014, accepted 23 October 2014)

Abstract: Amino ethyl-3-methylimidazolium tetrafluoroborate, [NH₃e-mim][BF₄], amino ethyl-3-methylimidazolium tetrafluoroborate, [OHe-mim][BF₄], and 2-hydroxyethylammonium lactate, [HOEAm], were selected and supported onto a variety of molecular sieves, NaY, USY, SAPO-34 and MCM-41, to prepare supported ionic liquids. It was found that [NH₃e-mim][BF₄]/NaY showed an excellent CO₂ adsorption performance, with an adsorption capacity of 0.11 mmol CO₂ g⁻¹. In this study, the optimal adsorption conditions and recyclability of [NH₃e-mim][BF₄]/NaY were investigated. The results showed that [NH₃e-mim][BF₄]/NaY showed good CO₂ adsorption under the conditions of 20 °C and 20 % loading of the IL. By vacuum heating, the CO₂ adsorption capacity reached 0.45 mmol CO₂ g⁻¹ in the fifth adsorption run but was reduced to 0.29 mmol CO₂ g in the tenth run. The structure and characterization of [NH₃e-mim][BF₄]/NaY were examined by FT-IR, XRD, SEM and TG-DSC. The TG-DSC results showed that the thermostability of NH₃e-mim][BF₄]/NaY was good below 50 °C.

Keywords: ionic liquid; molecular sieve; CO₂; adsorption capacity.

INTRODUCTION

It is well recognized that CO₂ is one of the most important greenhouse gases in the global warming phenomenon.^{1–3} Many technologies on CO₂ capture and storage (CCS) are being investigated to control CO₂ emissions.^{4–6} The employment of ionic liquids (ILs) for CO₂ capture was discussed in many reports and review articles.⁷ As a new type of green solvent,⁸ ILs have unique characteristics, such as wide liquid range, thermal stability, negligible vapor pressure and tunable physicochemical characteristics.^{9–11} However, the much discussed important drawbacks of ionic liquids are their high viscosity, slow adsorption rate and high costs, which has constrained the industrial application of ILs.¹² Scovazzo¹³ and

*Corresponding author. E-mail: ree_wong@hotmail.com
doi: 10.2298/JSC220214103Y

Hconich¹⁴ attempted to prepare ionic liquids supported on porous materials (SIL), and found that the porous material could well disperse ILs, improving the gas adsorption rate and reducing the amount of ILs used. Zhang *et al.*¹⁵ successfully prepared ionic liquids supported on SiO₂, with a CO₂ adsorption efficiency of 1.92 %. Fu *et al.*¹² investigated amino functionalized ionic liquids supported by Al₂O₃, SiO₂ and activated carbon, and found that the Al₂O₃-supported ionic liquids exhibited higher adsorption capacities for CO₂, with values of 0.359, 0.286 and 0.228 mmol g⁻¹ for [NH₃p-mim][Br]/Al₂O₃, [NH₃p-mim][PF₆]/Al₂O₃ and [NH₃p-mim][BF₄]/Al₂O₃, respectively. A molecular sieve was also investigated for CO₂ adsorption because of its large specific surface area and pore volume.¹⁶ Carbon dioxide capture by molecular sieve-supported ionic liquids is one of the promising methods. In this paper, ionic liquids supported on several molecular sieves were prepared. The optimal one was selected to optimize the adsorption conditions and investigate adsorbent reuse. Fourier transform infrared (FT-IR), powder X-ray diffraction (XRD), scanning electron microscopy (SEM), thermogravimetric analysis (TG) and differential scanning calorimetry (DSC) were used to characterize the obtained ionic liquids containing adsorbents.

EXPERIMENTAL

Chemical reagents and test equipment

Aminoethyl-3-methylimidazolium tetrafluoroborate ([NH₃e-mim][BF₄]), 1-hydroxy ethyl-3-methylimidazolium tetrafluoroborate ([OHe-mim][BF₄]) and 2-hydroxyethylammonium lactate ([HOEAm]), all A.R. grade, were supplied by Shanghai Chengjie Chemical Plant. The molecular sieves NaY, USY, SAPO-34, MCM-41, all A.R. grade, were received from the NanKai University Catalyst Institute. Ethanol, A.R. grade, was obtained from the Tianjin Fuyu Fine Chemical Co. Ltd. N₂ with a purity of 99.999 % and CO₂ with 10 % volume fraction, were supplied by Jinan Deyang Gas Co. Ltd.

Gas mass flow controllers, D08-1D/ZM for N₂ and D08-1F for CO₂, were supplied by Beijing Sevenstar Electronics Co. Ltd. Electric heating (DF-101S) and a rotary evaporator (Fre-52C) were produced by Henan Yuhua Instrument Co. Ltd. A portable IR CO₂ analyzer (GXH-3010E) was purchased from Beijing HuaYun Instrument Co. Ltd. A powder compressing machine (769YP-15A) was supplied by Tianjin Keqi Instrument Co. Ltd. A mortar, sieve and absorber were supplied by Jinan Bangen Instrument Co. Ltd.

Preparation of molecular sieve-supported ionic liquids

An IL (2 g) was dissolved in 75 mL of ethanol under vigorous stirring for 5 min, and the required quantity of molecular sieve was added to give the stipulated IL loading. The resulting mixture was stirred for 3 h at 20 °C, and then the ethanol was removed under vacuum in a rotary evaporator. The resulting solid was pressed into the form of a pellet using a powder compressing machine and then crushed into particles using a mortar. After screening of the 0.2–0.4 mm diameter particle using sieves, the molecular sieve-supported ionic liquid was obtained.

CO₂ adsorption and desorption test

The gas flow containing 10 % volume fraction of CO₂ was generated by mixing CO₂ at 8 mL min⁻¹ and N₂ at 192 mL min⁻¹. The system employed for the CO₂ adsorption experiments,

which included gas cylinders (CO₂, N₂), pressure regulators, gas mass flow controllers, absorber and CO₂ analyzer, is shown in Fig. 1. The absorber was a glass tube of inner diameter 1.0 cm with a gas dispersion orifice to support the fixed adsorbent bed. The temperature of the absorber was controlled by a thermostated water bath. CO₂ desorption was performed in a vacuum rotary evaporator operated at 100 °C for 3 h.

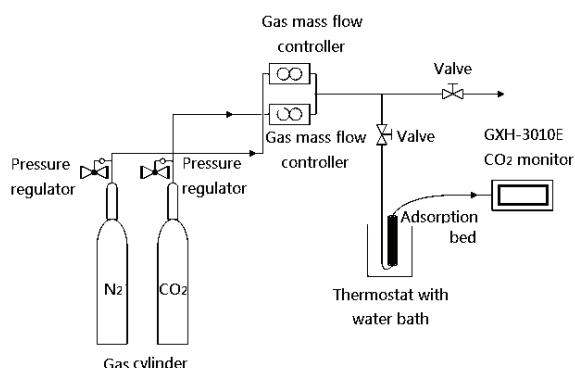


Fig. 1. Schematic presentation of the apparatus employed for the CO₂ adsorption experiments.
(IL loading on molecular sieve: 20 %, mass of SIL: 4g; concentration of CO₂: 3928 mg N m⁻³; T: 20 °C).

Characterization

The FT-IR spectra were recorded on a 5DXC IR spectrometer in the wavenumber range 4000 to 400 cm⁻¹ with a 2 cm⁻¹ resolution using 10 mg samples diluted with 150 mg KBr and pressed into a 13 mm pellet.

XRD measurements were performed on a Bruker D8 Advanced diffractometer with a Cu target, K_α-rays and a nickel filter. A scanning rate of 28 per minute in the 2θ scanning angle range of 3° and 70° was used.

The SEM pictures were acquired on a JEOL JSM-6700F microscope. Samples were coated with osmium. Particle size and size distribution analyses were performed on a dynamic light scattering (DLS) instrument.

TG and DSC analyses were realized on a SDT Q600 Universal V4.1D instrument (TA Instruments) under a dynamic N₂ atmosphere from room temperature to 700 °C at a heating rate of 10 °C min⁻¹.

RESULTS AND DISCUSSION

Adsorption performance of different supported ionic liquids

The three studied ILs, [NH₃e-mim][BF₄], [OHe-mim][BF₄] and [HOEAm], were supported on NaY, USY, SAPO-34 and MCM-41 at a loading of 20 % (w/w). The adsorption capacities of the prepared adsorbents (4 g) for CO₂ were determined at 20 °C. The performances of [NH₃e-mim][BF₄] supported on the different types of molecular sieves are shown in Fig. 2, from which it could be seen that [NH₃e-mim][BF₄]/NaY exhibited an excellent performance with a 24-min adsorption time, while the others had no obvious adsorption effect. The results

for [OHe-mim][BF₄] supported on the studied molecular sieves are shown in Fig. S-1 of the Supplementary material to this paper, showing that [OHe-mim][BF₄]/USY and [OHe-mim][BF₄]/MCM-41 had weak adsorption capacities with a 4-min effective adsorption time. The results for supported [HOEAm] are shown in Fig. S-1c, from which it could be observed that IL/NaY adsorbed CO₂ for only 5 min. The CO₂ adsorption by pure NaY was also tested and the result is presented in Fig. S-2 of the Supplementary material. Thus, NaY showed no obvious adsorption capacity. The corresponding adsorption capacities of the SIL samples and pure NaY were calculated and the results are presented in Table I. Thus that CO₂ adsorption capacity of [NH₃e-mim][BF₄]/NaY was the highest with a value of 0.11 mmol CO₂ g⁻¹ SIL, which is nearly three times higher than the corresponding value for [HOEAm]/NaY and five times than for [OHe-mim][BF₄]/USY.

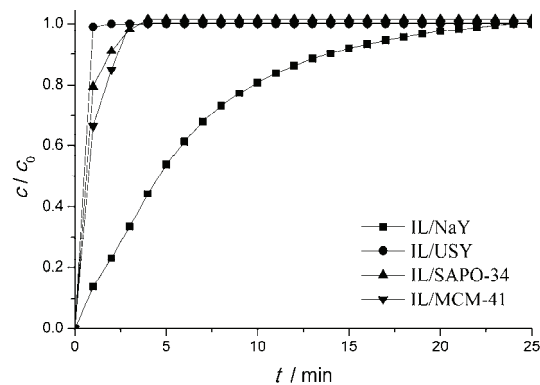


Fig. 2. Comparison of the CO₂ adsorption behavior of [NH₃e-mim][BF₄] supported on the different molecular sieves. Ionic liquid loading: 20 %, T: 20 °C; c_0 : initial concentration of CO₂ before the adsorbent (mol/mol); c : concentration of CO₂ after the adsorbent (mol/mol).

TABLE I. CO₂ adsorption capacities (mmol CO₂ g⁻¹) of the molecular sieves and supported ionic liquids

Support	IL			
	NaY	USY	SPA0-34	MCM-41
[NH ₃ e-mim][BF ₄]	0.108	0.009	0.009	0.017
[OHe-mim][BF ₄]	0.009	0.022	0.012	0.017
[HOEAm]	0.030	0.013	0.009	0.006
	0.010	—	—	—

The support and the ionic liquid jointly affect the CO₂ adsorption performance of SILs, with the effect of the later being predominant. Amino functional ionic liquids adsorb CO₂ by chemical action, which to better CO₂ adsorption performances than other ionic liquids adsorb by the formation of hydrogen bonds between networks and Lewis acid–base actions between CO₂ and the anion. The different adsorption mechanisms led to the different behavior of the three studied SILs. The specific surface area and pore structure of different supports also greatly influenced the CO₂ adsorption performance of the studied SILs. Thus, [NH₃e-mim][BF₄]/NaY adsorbed CO₂ by chemical action between –NH₂ and

CO₂, which was determined by the density of the electron cloud on the nitrogen atom of the –NH₂ group. Hence, it could be seen that CO₂ reacts with –NH₂ in NaY-supported ionic liquids easier and [NH₃e-mim][BF₄]/NaY was the best adsorbent of all the studied SILs.

Effect of temperature on the CO₂ adsorption capacity

[NH₃e-mim][BF₄]/NaY with a 20 % loading was chosen to investigate the CO₂ adsorption at 20, 30, 40 and 50 °C. The obtained results are shown in Fig. S-3 of the Supplementary material. From Fig. S-3, it could be seen that [NH₃e-mim][BF₄]/NaY exhibited the best adsorption at 20 °C and based on the presented results, the absorption capacities at the different temperatures were calculated. As can be seen in Table II, the value of the adsorption capacity at 20 °C was about two-times higher than those at the other temperatures. In addition, the CO₂ adsorption capacities at 30, 40 and 50 °C showed a slight decreasing tendency with increasing temperature. As a whole, considering also energy consumption, 20 °C could be recommended as the best adsorption temperature.

TABLE II. Relationships between CO₂ adsorption capacities (mmol CO₂/g) and temperature and IL loading amount for [NH₃e-mim][BF₄]/NaY

ILs loading, %	Temperature, °C			
	20	30	40	50
10	0.071	–	–	–
20	0.108	0.057	0.055	0.054
30	0.039	–	–	–

The temperature is one of the influential factors on adsorption capacity and penetration time. When the temperature increases, the adsorption capacity for CO₂ and adsorption time were significantly decreased. The reason may be that increasing temperature limited the adsorption capacity for CO₂ because the interaction between CO₂ and –NH₂ is weak and reversible and thus, higher temperatures lead to desorption of CO₂. Thus, the lowest temperature was advantageous to the adsorption of CO₂ on the surface of [NH₃e-mim][BF₄]/NaY.

Effect of the ILs loading amount on CO₂ adsorption capacity

[NH₃e-mim][BF₄]/NaY was selected to investigate the effect of IL loading on the adsorption of CO₂. Hence, [NH₃e-mim][BF₄]/NaY sorbents with IL loadings of 10, 20 and 30 % were prepared. The capacities of these SILs for CO₂ adsorption at 20 °C are presented in Fig. S-4 of the Supplementary material, from which it could be seen that the SILs with 10 and 30 % loadings reached saturation after 10 min, while the SIL with a 20 % loading attained saturation after 25 min. The CO₂ adsorption capacities calculated from the data presented in Fig. S-4 for the differently loaded ILs are listed in Table II. The SIL with a 30 % loading

had the lowest CO₂ capacity, less than half of that of the SIL with a 20 % loading. The reason lies in two aspects. On the one hand, increasing the loading with IL can enhance the adsorption; on the other hand, when reaching a certain degree of loading, the micropores of the support would be blocked, and hence the process of mass transfer during CO₂ adsorption would be markedly retarded. As a result, there should be a maximum loading corresponding to a higher CO₂ adsorption capacity. From this study, the favored loading was at around 20 %.

Recyclability of the adsorbent

To examine the recyclability of [NH₃e-mim][BF₄]/NaY, the CO₂ desorption test was performed in a rotary evaporator operated under vacuum at 100 °C for 3 h. As shown in Fig. 3, the CO₂ adsorption capacity increased during the first five repetitive runs and thereafter, gradually decreased during the following cycles. The adsorption capacity reached 0.45 mmol CO₂ g⁻¹ at the fifth run and decreased to 0.29 mmol CO₂ g⁻¹ at the tenth run. This may be the result of loss of crystal water during vacuum heating, which would change the morphology of the IL and increase the specific surface area of the adsorbent. With less retained water, the silica–alumina ratio would become higher, the SIL more alkaline and, consequentially, the CO₂ adsorption stronger. In addition, vacuum heating may increase the viscosity of the ILs supported on NaY. Fu¹² reported that the adsorption capacity for CO₂ could be improved by increasing the viscosity of supported ILs. The decline observed in the adsorption capacity is due to the leaking of IL during transport from the reactor to the regeneration container.

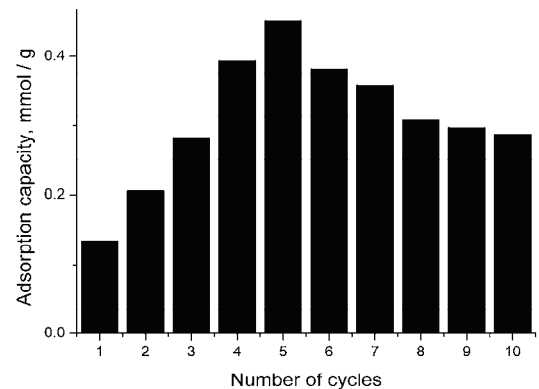


Fig. 3. Results of the recycling experiment for the adsorption of CO₂ by [NH₃e-mim][BF₄]/NaY.

Characterization of the adsorbent

A comparison of the FT-IR spectra of [NH₃e-mim][BF₄]/NaY, [NH₃e-mim][BF₄] and [NH₃e-mim][BF₄]/NaY after 10 cycles presented in Fig. 4. The comparison of FT-IR curves indicates that [NH₃e-mim][BF₄] was successfully supports on NaY. The imidazole ring skeleton stretching vibration band of [NH₃e-

-mim][BF₄] at 1571 cm⁻¹ was shifted to 1573 cm⁻¹ under the influence of NaY, and moved to 1575 cm⁻¹ after 10 cycles. This means that the level of conjugation changed. Combined with the way of the vibration spectra changed, it could be seen that the weak interaction between [NH₃e-mim][BF₄] and NaY led to a decrease in the level of conjugation, which could increase the functional site for CO₂ capture on [NH₃e-mim][BF₄]/NaY. Vacuum heating had the same effect of increasing the functional site for CO₂ capture by decreasing the conjugation, which is consistent with the experimental results of recycling the adsorbent.

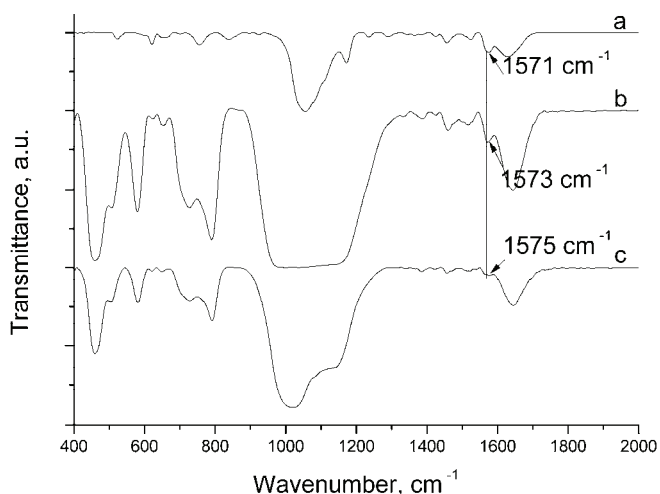


Fig. 4. FT-IR spectra of: a) [NH₃e-mim][BF₄]; b) [NH₃e-mim][BF₄]/NaY;
c) [NH₃e-mim][BF₄]/NaY after 10 cycles.

The XRD patterns for NaY, [NH₃e-mim][BF₄]/NaY, [NH₃e-mim][BF₄]/NaY with adsorbed CO₂, [NH₃e-mim][BF₄]/NaY after 4 and adsorption cycles are shown in Fig. 5. The XRD curves indicate that the diffraction peaks of NaY supported IL were much weak at 2θ values 6.1, 9.9, 11.8, 15.6, 18.6, 20.2, 24.8 and 26.9° but they reappeared after CO₂ adsorption. By comparing the XRD patterns (c), (d) and (e) in Fig. 5, it could be seen that the characteristic peaks of NaY gradually reappear on recycling [NH₃e-mim][BF₄]/NaY. The results may probably result from changes in the intensity of light reaching NaY, due to the presence of ILs. Actually, the structure of NaY remained intact. This demonstrates that [NH₃e-mim][BF₄] had been successfully supported on NaY, which was gradually reduced on recycling. In addition, the chemical properties of NaY were stable.

The morphologies of NaY and [NH₃e-mim][BF₄]/NaY were observed using scanning electron microscopy, and the images are shown in Fig. 6. NaY had a plain surface Fig. 6a, while [NH₃e-mim][BF₄]/NaY had a rough surface, with

tiny particles evenly distributed, Fig. 6b. This confirms the FT-IR and XRD results that $[\text{NH}_3\text{e-mim}][\text{BF}_4]$ had been successfully supported on NaY.

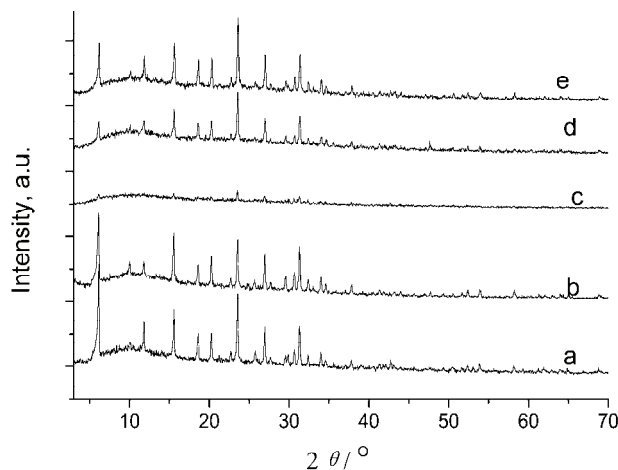


Fig. 5. The XRD patterns of: a) $[\text{NH}_3\text{e-mim}][\text{BF}_4]$ /NaY containing adsorbed CO_2 ; b) NaY; c) $[\text{NH}_3\text{e-mim}][\text{BF}_4]$ /NaY; d) $[\text{NH}_3\text{e-mim}][\text{BF}_4]$ /NaY after 4 cycles; e) $[\text{NH}_3\text{e-mim}][\text{BF}_4]$ /NaY after 10 cycles).

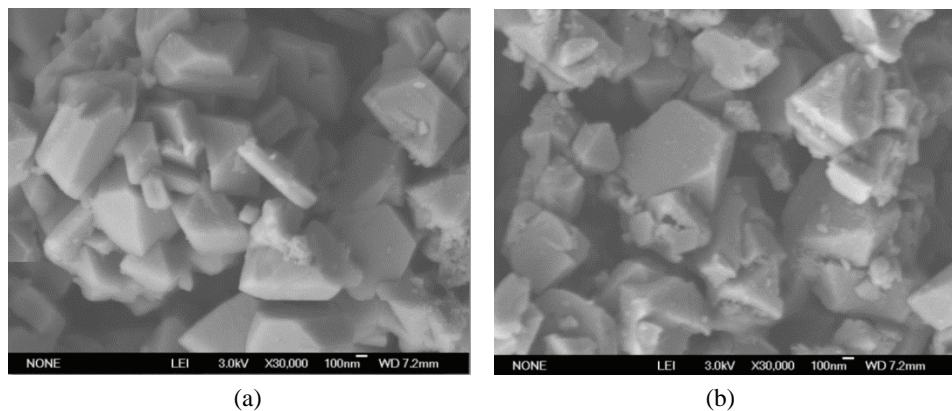


Fig. 6. Scanning electron microscopy (SEM) images of (a) NaY; (b) $[\text{NH}_3\text{e-mim}][\text{BF}_4]$ /NaY.

TG-DSC curves of $[\text{NH}_3\text{e-mim}][\text{BF}_4]$ and $[\text{NH}_3\text{e-mim}][\text{BF}_4]$ /NaY, both containing adsorbed CO_2 are shown in Fig. 7. As shown in Fig. 7b, the gradual weight loss of $[\text{NH}_3\text{e-mim}][\text{BF}_4]$ /NaY had three weight loss steps. The first step from 31 to 212 °C with a weight loss 7.18 % may result from the loss of small molecules and CO_2 desorption. The second one, assigned to the decomposition of SIL, appeared from 250 to 500 °C, with weight loss 14.42 %. Compared to the decomposition temperature from 300 to 400 °C of $[\text{NH}_3\text{e-mim}][\text{BF}_4]$ in Fig. 7a, the nature of the IL had changed. This proved that $[\text{NH}_3\text{e-mim}][\text{BF}_4]$ /NaY ads-

orbed CO₂ by chemical action. The observed decreased stability of SIL may be due to the alkaline characteristics of NaY promoting the decomposition of IL. At 50 °C, weight loss was about 5 %. This demonstrated that [NH₃e-mim][BF₄]/NaY was thermally stable during the adsorption experiments. The third decomposition step from 610 to 790 °C was due to further decomposition of the SIL.

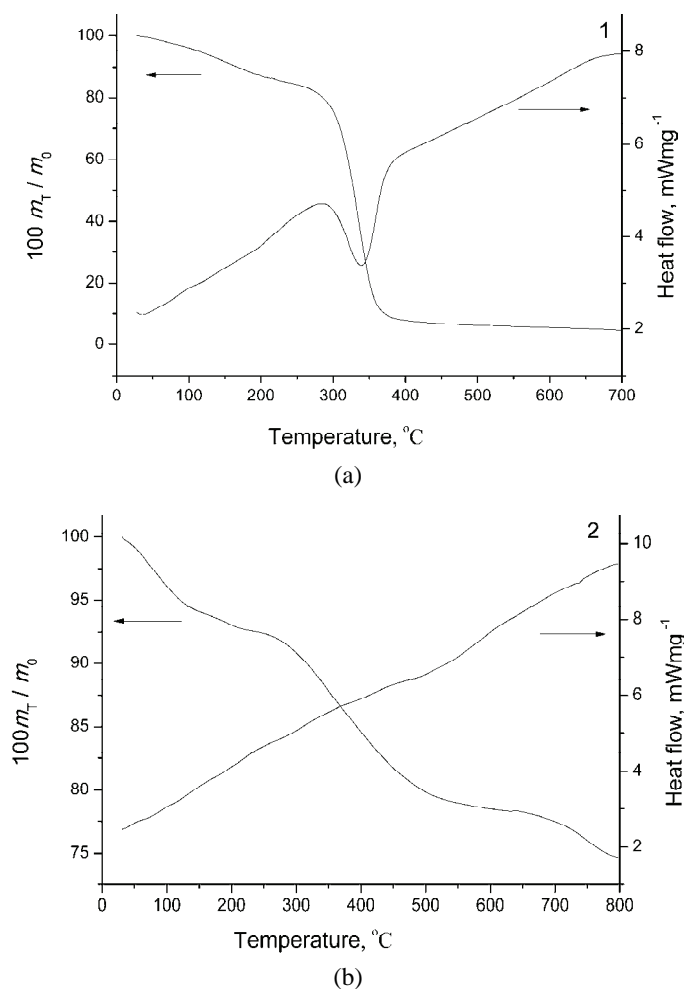


Fig. 7. TG-DSC curve of: a) [NH₃e-mim][BF₄] and b) [NH₃e-mim][BF₄]/NaY with adsorbed CO₂; m_T : mass at temperature T and m_0 : initial mass.

CONCLUSIONS

FT-IR, XRD, SEM and TG-DSC results demonstrated that molecular sieve-supported ionic liquids had been successfully prepared. [NH₃e-mim][BF₄]/NaY had an excellent CO₂ adsorption performance with adsorption capacity of 0.108

mmol CO₂ g⁻¹ SIL. Under the experimental temperatures, the adsorbent has good thermal stability. By optimizing the adsorption conditions, the optimal temperature was found to be 20 °C, and the optimal IL loading was 20 %. In the investigation of the recyclability of the adsorbent, the CO₂ adsorption capacity was found to increase in the first five repeated runs and gradually decrease with subsequent recycling. Vacuum heating could improve the CO₂ adsorption capacity of [NH₃e-mim][BF₄]/NaY.

SUPPLEMENTARY MATERIAL

CO₂ adsorption behaviors of supported ionic liquids and NaY, Figs. S-1 and S-2, as well as the effects of temperature and ILs loading on CO₂ adsorption by [NH₃e-mim][BF₄]/NaY, Figs. S-3 and S-4, are available electronically from <http://www.shd.org.rs/JSCS/>, or from the corresponding author on request.

Acknowledgments. We wish to thank the PetroChina Innovation Foundation (2013D-5006-0507) and Jinan R&D Innovation Project (201102041) for financial support.

ИЗВОД
ЈОНСКЕ ТЕЧНОСТИ НА НОСАЧУ ОД МОЛЕКУЛСКИХ СИТА КАО ЕФИКАСНИ
АДСОРБЕНСИ ЗА CO₂
NA YANG¹ и RUI WANG²

¹*School of Environmental Science and Engineering, Shandong University, Jinan 250100, Shandong, China*
²*School of Environmental Science and Engineering, Shandong University, Jinan 250100, Shandong, China*

Одабране су јонске течности [NH₃e-mim][BF₄], [OHe-mim][BF₄] и [HOEAm] и нанесене на молекулска сита NaY, USY, SAPO-34 и MCM-41 као носаче. Нађено је да [NH₃e-mim][BF₄]/NaY има одличне перформансе у адсорпцији CO₂, са адсорpcionим капацитетом од 0,108 mmol CO₂ g⁻¹. Испитани су оптимални адсорpcionи услови и рециклабилност [NH₃e-mim][BF₄]/NaY. Резултати показују да [NH₃e-mim][BF₄]/NaY добро адсорбује CO₂ при 20 °C и 20 % садржаја јонске течности. Загревањем у вакууму адсорpcionи капацитет CO₂ достиже 0,451 mmol CO₂ g⁻¹ у петом пролазу, а смањује се на 0,29 mmol CO₂ g⁻¹ на десетом пролазу. Одређивање структуре и карактеризација [NH₃e-mim][BF₄]/NaY је урађена FT-IR, XRD, SEM и TG-DSC методама. TG-DSC анализа је показала добру термичку стабилност [NH₃e-mim][BF₄]/NaY на температурата испод 50 °C.

(Примљено 22. фебруара, ревидирано 29. септембра, прихваћено 23. октобра 2014)

REFERENCES

1. D. L. Cui, L. Ma, *Huaxue-gongye-yu-gongcheng* **43** (2012) 12 (in Chinese)
2. F. Yang, R. Wang, *Meitan Xuebao* **38** (2012) 1060 (in Chinese)
3. K. L. In, Y. H. Ju, G. C. Chen, *Catal. Today* **148** (2009) 389
4. Z. H. Sun, Q. Wang, M. X. Song, *Chemical Industry and Engineering Progress* **32** (2013) 1666
5. X. K. Jian, S. C. Liu, Y. Bian, *Biomass Chem. Eng.* **46** (2012) 20
6. T. Yang, J. Bi, K. H. Guo, *CIESC J.* **63** (2012) 3150
7. M. Hasib-ur-Rahman, M. Siaj, F. Larachi, *Chem. Eng. Process.* **49** (2010) 313
8. S. Subbiah, S. Venkatesan, T. Ming-Chung, *Molecules* **14** (2009) 3780
9. J. Sun, W. G. Cheng, W. Fan, *Catal. Today* **148** (2009) 361

10. R. LPN, L. JNC, E. JMSS, *J. Phys. Chem., B* **109** (2005) 040
11. J. L. Anderson, D. M. Armstrong, *Anal. Chem.* **75** (2003) 4851
12. G. H. Fu, G. X. Lv, J. T. Ma, *Fenxi Ceshi Jishu yu Yiqi* **19** (2013) 41 (in Chinese)
13. P. Scovazzo, J. Kieft, D. A. Finan, *J. Membr. Sci.* **238** (2004) 57
14. H. Jeffery, M. Christina, P. Hennry, *J. Membr. Sci.* **298** (2007) 41
15. H. Zhang, J. M. Zhu, K. G. He, *Modern Chem. Ind.* **31** (2011) 45
16. L. Zhou, J. Fan, G. Cui, *Green Chem.* **16** (2014) 4009.